Table 3
Treatment methods of 194 keloids.

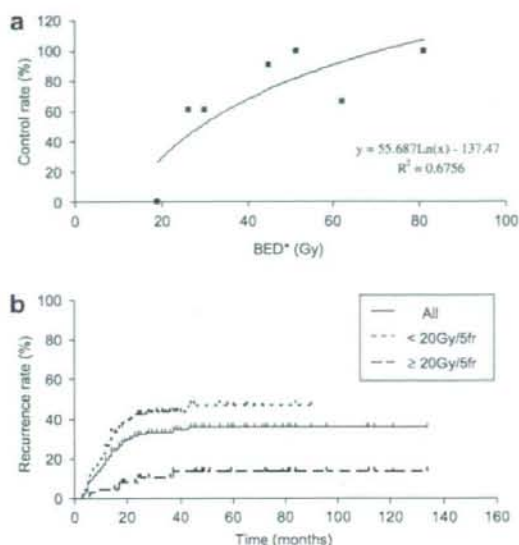|	Number of fractions	Number of keloids
Fraction dose (Gy)		
2	8	3
2	10	5
2	13	4
2	20	2
2.5	8	1
2.5	10	1
2.5	14	1
3	6	1
3	10	13
3	12	1
3	13	1
4	4	128
4	5	4
4	6	24
5	4	1
5	5	1
5	6	2
5	8	1
Radiation source		
X-ray		
55 kVp		74
100 kVp		114
Electron		
4 MeV		4
6 MeV		2
Total treatment time (days)		
5–9		106
10–14		47
15–19		11
20–24		9
25–29		12
30–34		2
35–39		5
40≤		2
Median 9 days		
Interval between operations and irradiations (days)		
<2		22
2–5		66
6–9		33
10–14		37
15–19		14
20–24		5
25–29		12
30≤		5
Median 7 days		
Total		194

Fig. 1. (a) Control rate of keloids as function of the biologically effective dose (BED). There was a significant correlation between the control rate and biologically effective dose (BED*). *BED calculation according to Kal et al. [13]. (b) Long-term recurrence rate in post-operative radiotherapy according to the total dose. The recurrence rate ≥20 Gy in five fractions was significantly lower than that with <20 Gy in five fractions. **Significant (logrank test).

ysis, the factors of elderly patients, minor etiology, and of previous treatment remained significant.

There were no cases of serious toxicity, defined as World Health Organization grade 3 or higher. There were no cases of malignant tumors being generated at the keloid site.

Discussion

Consistent reliable control of keloids using postoperative irradiation has been reported by many authors [10–12,14–18]. There is a controversy concerning the total dose in these previous reports, as well as whether the treatment was given in one fraction or in several fractions. There was no consensus with respect to the total Q2 dose and dose fractionation in the treatment of keloids. A summary of the local control rates of postoperative radiotherapy of keloids is shown in Table 7 [1,10–12,14,19–27].

The mechanism of the radiotherapeutic prevention of keloids is still poorly understood. One of the proposed mechanisms is the control of collagen synthesis by eliminating abnormally activated fibroblasts and promoting the existing normal fibroblasts [28]. In vitro experimental evidence suggests that a fraction dose of about 5 Gy may be effective in inducing radiolysis of fibroblasts [18]. Using in vivo experiments with rat skin, the radiolytic process of fibroblasts starts minimally from 0.5 to 2.5 Gy. Recoiled collagen fibrils return to their normal shape and size 4–6 weeks after radiotherapy [18].

However, a higher dose seems necessary in the clinical situation. Brown and Bromberg identified a minimum isoeffect time–dose line for reliable postoperative keloid control at 9–10 Gy delivered over 1 week or 15 Gy over 2 weeks. With BED above this level, 100% control was achieved [29]. Edsmyer et al. confirmed the threshold dose for reliable control as 12–14 Gy in single fraction by X-ray in the postoperative setting and it is

for doses lower than 20 Gy in five fractions and for women. In multivariate analysis, these factors remained significant.

The positive adverse effect rate was 19% (36/194) in all lesions, and univariate and multivariate analyses of adverse effect rate are shown in Table 6. Univariate analysis showed that the adverse effect rate was significantly higher for elderly patients (≥25 years old), minor etiology, large keloids (longer axis ≥5 cm), previous treatment, use of high voltage X-rays (100 kVp) or electrons, and total dose of 20 Gy in five fractions or higher. In multivariate analysis, the factors of elderly patients, minor etiology, and of previous

Table 4
Symptomatic relief.

Symptomatic relief	Pain lesions (%)	Itching lesions (%)
None	116	65
Relief	75/78 (96)	118/129 (91)
No change	3/78 (4)	11/129 (9)
Worse	0	0
Total	194	194

4   *Dose optimization of keloids*

Table 5
Long-term control of 194 keloids.

Factor	Category (n)	Recurrence rate (%)	Univariate analysis	Multivariate analysis
Gender	Male (85)	25	$p = 0.031^*$	$p = 0.0069^{**}$
	Female (109)	39		
Age	<25 y.o. (132)	38	$p = 0.083$	$p = 0.42$
	≥25 y.o. (62)	23		
Site	Without high tension (45)	29	$p = 0.48$	$p = 0.50$
	With high tension (149)	34		
Etiology	Minor (109)	37	$p = 0.23$	$p = 0.075$
	Major (85)	28		
Longer axis	<5 cm (74)	36	$p = 0.53$	$p = 0.75$
	≥5 cm (120)	31		
Previous treatment	– (137)	32	$p = 0.62$	$p = 0.97$
	57	35		
Affliction time	<5 years (73)	38	$p = 0.17$	$p = 0.063$
	≥5 years (121)	30		
Interval from operation	<6 days (88)	34	$p = 0.83$	$p = 0.62$
	≥6 days (106)	32		
Source	55 kvp (74)	37	$p = 0.54$	$p = 0.15$
	100 kvp, electron (120)	31		
Total dose	<20 Gy (132)	43	$p < 0.0001^*$	$p = 0.0002^{**}$
	≥20 Gy (62)	11		

* Significant (logrank test).
** Significant (Cox proportional hazard model).

probably best to give the radiotherapy immediately after the excision [24,30]. Van den Brenk et al. reported that possible skin necrosis after single-fraction irradiation encouraged fractionated radiotherapy schedules, regardless of the dose [31]. According to Kal et al. [13], biologically effective doses (BEDs) of the various irradiation regimens were calculated using the linear–quadratic concept, and the recurrence rate decreased as a function of BED in the range of BED above 10 Gy. At a BED higher than 30 Gy, the recurrence rate was lower than 10%.

Thus, the dose–response relationship in the treatment of postoperative keloids had been reported in several previous studies. Also, in our study, we found a significant correlation between the recurrence rate and the total dose. The recurrence rate was 11% at a total dose of 20 Gy in five fractions or higher, while 43% under 20 Gy in five fractions. The recurrence rate was 33% for all lesions evaluated in this study, which was comparable to that of the previous studies (Table 7); however, the recurrence rate for lesions treated with the schedule of 20 Gy in five fractions, equivalent to a BED of 30 Gy according to Kal et al. [13], was 18%. It was suggested that this dose fraction was necessary and sufficient for keloid control. On the other hand, the positive adverse effect rate was also dose-dependent; 44% at a total dose of 20 Gy in five fractions or higher, while 7% at under 20 Gy; however, the positive adverse effect rate for the schedule of 20 Gy in five fractions was

Table 6
Adverse effects of 194 keloids.

Factor	Category (n)	Adverse effect (%)	Univariate analysis	Multivariate analysis
Gender	Male (85)	22	$p = 0.30$	$p = 0.56$
	Female (109)	16		
Age	<25 y.o. (132)	13	$p = 0.0057^*$	$p = 0.0018^{**}$
	≥25 y.o. (62)	31		
Site	Without high tension (45)	11	$p = 0.092$	$p = 0.61$
	With high tension (149)	21		
Etiology	Minor (109)	26	$p = 0.0047^*$	$p = 0.032^{**}$
	Major (85)	9		
Longer axis	<5 cm (74)	9	$p = 0.041^*$	$p = 0.64$
	≥5 cm (120)	24		
Previous treatment	–(137)	24	$p = 0.0071^*$	$p = 0.0089^{**}$
	+(57)	5		
Affliction time	<5 years (73)	12	$p = 0.25$	$p = 0.33$
	≥5 years (121)	22		
Interval from operation	<6 days (88)	24	$p = 0.53$	$p = 0.70$
	≥6 days (106)	15		
Source	55 kvp (74)	5	$p = 0.0037^*$	$p = 0.13$
	100 kvp, electron (120)	27		
Total dose	<20 Gy (132)	7	$p < 0.0001^*$	$p = 0.039^{**}$
	≥20 Gy (62)	44		

* Significant (logrank test).
** Significant (Cox proportional hazard model).

RADION 4543

13 January 2009 Disk Used

ARTICLE IN PRESS

No. of Pages 6, Model 5G

T. Sakamoto et al. / Radiotherapy and Oncology xxx (2009) xxx–xxx

5

Table 7
Summary of local control rates of post-operative radiotherapy of keloids.

Author (Year)	Number of cases	Median follow-up time (months)	Treatment dose (Gy)	Number of fraction	Radiation type	Interval between operation and irradiation (days)	Local control rate (%)	BED (Gy)
Cosman (1961)	94	12	7.7*	4	Deep X	14–42	69	10.6*
Craig (1965)	16	12	7.7*	1	100 kVX	<2	87	16.2*
King (1970)	32	Unknown	9.6–28.8*	1–3	1–3 MeV–E	<1	74.1	Mean 29.7*
Mathangi-Ramakrishan (1974)	36	Unknown	15.4*	2–3	Deep X	<1	98	Mean 34.7*
Edsmyr (1975)	103	2	4.8–23*	1–14	45,100 kVX	<8	80	Mean 28.6*
Levy (1976)	35	6	14.4–17.3*	5–6	100 kVX	1–2	88	Mean 23.8*
Ollstein (1981)	68	12	14.4*	3	100 kVX	<1	79	25.1*
Enhamre (1983)	62	6	9.6–14.4*	1–3	20 kVX	1–14	88	Mean 32.7*
Borok (1988)	375	Unknown	3.8–15.4*	Variety (3–4**)	X, E	<2**	97.6	15.9–21.3**
Kovalic (1989)	113	117	3–20	1–5	X 89% Co, E 11%	1–21	73	Mean 18.8
Doornbos (1990)	263	12	4.5–18	2–4	120 kVX	3–10	85.7***	24.1***
Escarmant (1993)	570	15	8–30	1	LDR	<2	79	Mean 55.8
Norris (1995)	24	24	8–12*	1–3	E 5 100 kV X 19	1–68	47	Mean 17.8*
Ogawa (2003)	14	24	15	3	4 MeV–E	<2	67	22.5
Current study	194	36	16–40	4–20	55, 100 kVX 188 4, 6 MeV–E 6	1–72 (mean 9.7)	67	Mean 33.5

LDR, low dose rate 192Ir; X, X-ray beam; E, electron beam; Co, cobalt beam.
* For BED calculation we applied 1R = 0.96 cGy.
** After 1981, radiation technique was standardized to 1200–1600 rad in three to four fractions.
*** 15 Gy in three fractions.

not very high (18%). Thus, we considered this dose fraction to be acceptable regarding morbidity. Therefore, since 1995, we have employed a schedule of 20 Gy in five fractions for almost all newly treated postoperative keloids, in the expectation of preserving low morbidity without compromising the control rate.

In the prognostic analysis of this study, female gender was associated with a higher recurrence rate. Previous studies had scarcely demonstrated a correlation between gender and recurrence. The cure of hypertrophic scars is occasionally protracted in young women, maybe because the propagation of fibroblasts is exceeded during recovery at the wound [32,33]. In addition, elderly patients and previous treatment were associated with a higher positive adverse effect rate. Aging and treatment history may cause potentially enhanced radiosensitivity of normal cutaneous tissue, possibly resulting in greater adverse effects.

The influence of the interval between excision and the commencement of radiotherapy on recurrence remains controversial. Cosman et al. [1,34] and Hintz [35] suggested an advantage of the rapid initiation of postoperative irradiation. In contrast, Enhamre and Hammar [36] found no association with the results and interval time between excision and irradiation. In our study, we did not find a significant correlation between the recurrence rate and the interval between excision and radiotherapy, possibly because its influence may have been masked by the large variation of the dose fractionation. This should be further studied using a uniform dose fractionation schedule.

The total radiation dose correlated significantly both with the recurrence rate and with the positive adverse effect rate. It was suggested that 20 Gy in five fractions was a recommendable dose fractionation schedule in the expectation of preserving low morbidity without compromising the control rate.

Acknowledgement

References

[1] Cosmann B, Crikelar GF, Ju DMC, Gaulin JC, Lattes R. The surgical treatment of keloids. Plas Reconstr Surg 1961;27:335–58.
[2] Kiil J. Keloids treated with topical injections of triamcinolne acetonide. Scand J Plast Reconstr Surg 1977;11:169–72.
[3] Apfelberg DB, Maser MR, White DN, Lash H. Failure of carbon dioxide laser excision of keloids. Lasers Surg Med 1989;9:382–8.
[4] Sherman R, Rosenfeld H. Experience with the Nd YAG laser in the treatment of keloid scars. Ann Plast Surg 1988;21:231–5.
[5] Mercer NS. Silicone gel in the treatment of keloid scars. Br J Plast Surg 1989;42:83–7.
[6] Panabiere-Cataing MH. Retinoic acid in the treatment of keloids. J Dermatol Surg Oncol 1988;14:1275–6.
[7] Ohmori S. Effectiveness of silastic sheet coverage in the treatment of scar keloid (hypertrophic scar). Aesthetic Plast Surg 1988;12:95–9.
[8] Sclafani AP, Gordon L, Chadha M, et al. Prevention of earlobe keloid recurrence with postoperative corticosteroid injections versus radiation therapy: a randomized, prospective study and review of the literature. Drmatol Surg 1996;22:569–74.
[9] Guix B, Henriquez I, et al. Treatment of keloids by high-dose-rate brachytherapy: a seven-year study. Int J Radiat Oncol Biol Phys 2001;50(1):167–72.
[10] Borok TL, Bray M, Sinclair I, et al. Role of ionizing irradiation for 393 keloids. Int J Radiat Oncol Biol Phys 1988;15:865–70.
[11] Kovalic JJ, Perez CA. Radiation therapy following keloidectomy: a 20-year experience. Int J Radiat Oncol Biol Phys 1989;17:77–80.
[12] Escarmant P, Zimmermann S, Amar A, et al. The treatment of 783 keloid scars by iridium 192 interstitial irradiation after surgical excision. Int J Radiat Oncol Biol Phys 1993;26:245–51.
[13] Kal HB, Veen RE. Biologically effective dose of postoperative radiotherapy in the prevention of keloids. Strahlenther Onkol 2005;181:717–23.
[14] Doornbos JF, Stoffel TJ, Hass AC, et al. The role of kilovoltage irradiation in the treatment of keloids. Int J Radiat Oncol Biol Phys 1990;18:833–9.
[15] Clavere P, Bedane C, Bonnetblanc JM, et al. Postoperative interstitial radiotherapy of keloids by iridium 192: a retrospective study of 46 treated scars. Dermatology 1997;195:349–52.
[16] Caccialanza M, Piccinno R, Schiera A. Postoperative radiotherapy of keloids: a twenty-year experience. Eur J Dermatol 2002;12:58–62.
[17] Dinh Q, Veness M, Richards S. Role of adjuvant radiotherapy in recurrent earlobe keloids. Australas J Dermatol 2004;45:126–62. Q3
[18] Malaker K, Vijayraghavan K, Hodson I, et al. Retrospective analysis of treatment of unresectable keloids with primary radiation over 25 years. Clin Oncol (R Coll Radiol) 2004;16:290–8.
[19] Norris JE. Superficial X-ray therapy in keloid management: a retrospective study of 24 cases and literature review. Plast Reconstr Surg 1995;95:1051–5.
[20] Cohen IK, Peacock EE. Keloids and hypertrophic scars. In: McCarthy JG, editor. Plastic surgery. Philadelphia: W.B. Saunders Company; 1990. p. 732–47.
[21] Craig RDP, Pearson D. Early post-operative irradiation in the treatment of keloid scars. Br J Plast Surg 1965;18:369–76.
[22] King GD, Salzman FA. Keloid scars; analysis of 89 patients. Surg Clin North Am 1970;50:595–8.
[23] Mathangi-Ramakrishnan K, Thomas KP, Sundararajan CR. Study of 1000 patients with keloids in South India. Plast Reconstr Surg 1974;53:276–86.
[24] Edsmyr F, Larsson LG, Onyango J, et al. Radiotherapy in the treatment of keloids in East Africa. East Afr Med J 1973;50:457–61.
[25] Levy DS, Salter MM, Roth RE. Postoperative irradiation in the prevention of keloids. Am J Roentgenol 1976;127:509–10.
[26] Ollstein RN, Siegel HW, Gillooley JF, et al. Treatment of keloids by combined surgical excision and immediate post-operative X-ray therapy. Ann Plast Surg 1981;7:281–5.

6   *Dose optimization of keloids*

[27] Ogawa R, Mitsuhashi K, Hyakusoku, et al. Postoperative electron-beam irradiation therapy for keloids and hypertrophic scars: retrospective study of 147 cases followed for more than 18 months. Plast Reconstr Surg 2003;111:547–53.

[28] Stadelmann WK, Digenis AG, Tobin GR. Physiology and healing dynamics of chronic cutaneous wounds. Am J Surg 1998;176:26S–38S.

[29] Brown JR. Bromberg JH: preliminary studies on the effect of time–dose patterns in the treatment of keloids. Radiology 1963;80:298–300.

[30] Edsmyr F, Larsson LG, Onyango J, et al. Radiation therapy in the treatment of keloids in East Africa. Acta Radiol Ther Phys Biol 1974;13:102–6.

[31] Van Den Brenk HA, Minty CC. Radiation in the management of keloids and hypertrophic scars. Br J Surg 1960;47:595–605.

[32] Epstein Jr EH, Munderloh NH. Isolation and characterization of CNBr peptides of human $[\alpha1(III)]_3$ collagen and tissue distribution of $[\alpha1(I)]_2$–$\alpha2$ and $[\alpha1(III)]_3$ collagens. J Biol Chem 1975;250:9304–12.

[33] Hayakawa T, Hashimoto Y, Myokei Y, et al. Changes in type of collagen during the development of human postburn hypertrophic scars. Clin Chim Acta 1979;93:119–25.

[34] Cosman B, Wolff M. Bilateral earlobe keloids. Plast Reconstr Surg 1974;53:540–3.

[35] Hintz BL. Radiotherapy for keloid treatment. J Natl Med Assoc 1973;65:71–5.

[36] Enhamre A, Hammar H. Treatment of keloids with excision and postoperative X-ray irradiation. Dermatologica 1983;167:90–3.

ORIGINAL ARTICLE

SuYu Zhu · Takashi Mizowaki · Yoshiki Norihisa
Kenji Takayama · Yasushi Nagata · Masahiro Hiraoka

Comparisons of the impact of systematic uncertainties in patient setup and prostate motion on doses to the target among different plans for definitive external-beam radiotherapy for prostate cancer

Abstract

Background. We aimed to compare the impact of systematic uncertainties in patient setup and prostate motion on three different external-beam radiotherapy protocols for prostate cancer.

Methods. To simulate possible near-maximum systematic errors, the isocenter position was shifted to eight points with ±1.65 SD of the integrated uncertainty value along each axis that was expected to include 5%–95% of the total systematic uncertainties in each direction. Five cases were analyzed for the three plans: an old three-dimensional conformal radiotherapy (3D-CRT) protocol (four-field plus dynamic arc), a new 3D-CRT protocol (dynamic arc), and an intensity-modulated radiotherapy (IMRT) protocol, respectively.

Results. The averaged percentage volume covered by more than 95% of the prescription dose (V95) of the clinical target volume (CTV) for the original plans was 100% for all protocols. After simulating the errors, V95 of the CTV for IMRT cases was maintained at 100%. On the other hand, these values for the new and old 3D-CRT protocols were 93.1% and 63.2%, respectively. The values for the percentage prescription dose received by at least 95% volume (D95) of the CTV for the original plans were 100%, 98.4%, and 97.6% for the IMRT, new 3D-CRT, and old 3D-CRT plans, respectively. However, when the effects of the systematic errors were taken into consideration, the net decreases in the D95 values were 0.3%, 4.3%, and 8.1%, respectively.

Conclusion. The current IMRT protocol is considered to successfully compensate for systematic uncertainties. In contrast, the multi-leaf collimator (MLC) margins set for the old 3D-CRT protocol were not enough to ensure the actual delivery of the prescription dose to the CTV. Therefore, it is very important to include these issues in the plan design in the interpretation of clinical outcomes.

Key words Systematic uncertainties · Dynamic-arc 3D-CRT · IMRT · Prostate cancer

Introduction

Geometrical uncertainties in radiotherapy can cause differences between the planned and the actually delivered dose distribution. The uncertainties mainly consist of setup deviation and internal organ motion. Both uncertainties can be separated into random and systematic components.

Setup error and organ motion in external-beam radiotherapy for prostate cancer have been widely investigated using megavoltage film or an electronic portal image device (EPID),[1-3] sequential computed tomography (CT) scans,[4-9] implanted radiopaque markers,[3,10-12] and a B-Mode Acquisition and Targeting System (BAT).[13,14] With better understanding of these uncertainties, the margin added to the clinical target volume (CTV) to create the planning target volume (PTV) is gradually reduced in conformation therapy to reduce the irradiated dose and volume to the organs at risk and to increase the dose to the CTV. However, a PTV margin that is too small will result in geometrical errors at some or even all treatment fractions. It has therefore become increasingly important to quantify and verify whether the applied margins can account for the uncertainties. Among the components of errors, random errors mainly result in blurring the dose distribution.[15,16] This blurring due to the random errors tends to have a relatively small impact on doses to the target and normal structures.[15] On the other hand, systematic errors have a much larger potential to cause significant underdosing or overdosing to both the target and normal structures.[8,15,17]

Therefore, the present study was designed to compare the effect of systematic components of setup errors and prostate motion on prostate dose coverage among three

S.Y. Zhu · T. Mizowaki (✉) · Y. Norihisa · K. Takayama · Y. Nagata · M. Hiraoka
Department of Radiation Oncology and Image-applied Therapy, Graduate School of Medicine, Kyoto University, 54 Shogoin-Kawahara-cho, Sakyo, Kyoto 606-8507, Japan
Tel. +81-75-751-3762; Fax +81-75-771-9749
e-mail: mizo@kuhp.kyoto-u.ac.jp

Table 1. Summary of the three definitive radiotherapy protocols

Protocols	Fields	PTV margins (mm)	MLC and jaw margins (mm)	Setup	Dose (Gy)	Dose prescription
Old 3D-CRT	MLC- Shaped box	Not created	Superior: 12 Inferior: 12 Lateral: 7	Supine without fixation	46	Isocenter
	Dynamic arcs	Not created	Superior: 12 Inferior: 12 Lateral: 7		24	Isocenter
New 3D-CRT	Dynamic arcs	9 (6, Posterior)	Superior: 8 Inferior: 8 Lateral: 3	Supine without fixation	74	Isocenter
IMRT	215° 280° 0° 75° 145°	9 (6, Posterior)	Dynamic MLC, automatic defined: 7–9 mm	Prone with hip fixation	74	D95 of the PTV = 95% (>90%)

PTV, planning target volume; MLC, multi-leaf collimator

definitive external-beam radiotherapy plans for localized prostate cancer, and hence to verify whether the margins set for the three protocols could account for those uncertainties.

Patients, materials, and methods

Description of the three definitive radiotherapy protocols

Since 1998, three definitive radiotherapy protocols have been applied to the treatment of localized prostate cancer at our institute. They are the old three-dimensional conformal radiotherapy (3D-CRT), new 3D-CRT and intensity-modulated radiotherapy (IMRT) protocols, respectively. Details of each planning protocol have already been reported.[18] Briefly, in the old 3D-CRT protocol, a planning target volume (PTV) was not created. A multileaf collimator (MLC) with a leaf width of 1 cm was directly fitted to the clinical target volume (CTV), which is the prostate, with margins. Forty-six Gy in 23 fractions was given, using the four-field box technique with MLC conformation to the CTV, followed by an additional 24 Gy in 12 fractions with the dynamic-arc conformal technique. In the four-field irradiation, MLC or jaw edges were placed directly on the CTV with margins of 12 mm in superior/inferior directions and 7 mm in the remaining directions based on the beam's eye view of each field. If a part of the posterior rectal wall was included in the lateral opposing fields, the MLC positions were manually adjusted to completely shield the posterior wall from the irradiated area by the bilateral fields. In the dynamic-arc conformal radiotherapy, two lateral arcs with 100° of rotation (from 36° to 136°, and from 226° to 326°) were used with dynamic conformal fitting of MLCs to the CTV with a 7-mm margin. In the new 3D-CRT and IMRT protocols, PTV was created by adding a 9-mm margin to the CTV, except for the posterior rectal-prostate interface, where a 6-mm margin was applied. For the new 3D-CRT protocol, two lateral dynamic arcs with 100° of rotation (from 36° to 136° and from 226° to 326°) were used by dynamic conformal fitting of MLCs to the PTV, in which a 3-mm margin was generally placed from the edge of the PTV to the tips of the MLCs. With respect to the superior

and inferior directions, jaws were fitted with an 8-mm margin to the PTV to ensure 95% dose at the edge of the PTV. For the IMRT protocol, inverse optimization was used to achieve the goal that the percentage prescription dose received by at least 95% volume (D95) of the PTV should generally exceed 95% (at least 90%). The old and new 3D-CRT techniques are performed with the patients in the supine position without any fixation, while IMRT is applied with the patients immobilized in the prone position, using thermoplastic shells fixed to a rigid pelvic board Hip Fix (MedTec, Inc, Orange City, IA, USA) extending from the mid-thigh to the upper third of the leg and with the feet being put on a cushion support. Details of the three protocols are summarized in Table 1.

Institutional measured uncertainties

From March 2001 to March 2002, a study was conducted to measure setup errors and prostate motion using serial computed tomography (CT) verification scans. Ten patients in the supine position, without fixation devices, and eight patients in the prone position, fixed with a set of thermoplastic shells, were enrolled in the study. Three CT verification scans were performed at 2-week intervals for the whole course of radiotherapy for each patient. CT scans were conducted with the same conditions as the simulation scans; that is, empty rectum and moderately dilated bladder (0.5–1.0 h after micturition). The three serial CT scan images were registered to the simulation CT scan images using the same Digital Imaging and Communications in Medicine (DICOM) coordinates. The prostate was contoured and the center was reconstructed. Four reference points on the pelvic bony structure (two on the innermost edge of the femoral head, one on the anterior-superior edge of the coccyx, and one on the posterior-superior edge of the pubic symphysis) were chosen to calculate the relative position of the prostate along three axial directions. Compared with the relative prostate position on the simulation CT images, the systematic and random prostate motions were calculated. The systematic displacement was taken to be the difference between the prostate position in the planning scan and the mean position as calculated from the three treatment scans, and the random displacements were calculated as the devia-

Table 2. Institutional data of systematic uncertainties and the integration used for simulations

	1 SD of systematic setup error	1 SD of systematic prostate motion	1 SD of integrated systematic error $(\Sigma\delta^2 = IM^2 + SM^2)$	Simulating value 1.65 SD (5%–95% CI)
	Prone Supine	Prone Supine	Prone Supine	Prone Supine
LR (mm)	1.6	0.8	1.8	3.0
	3.0	0.9	3.1	5.1
AP (mm)	1.6	2.1	2.6	4.3
	3.4	3.7	5.0	8.3
CC (mm)	3.1	3.1	4.4	7.3
	3.2	1.7	3.6	5.9

LR, Left-right; AP, anterior-posterior; CC, cranial-caudal; δ, total margin; IM, internal margin; SM, setup margin; CI, confidence interval

tion of the prostate position in each treatment scan from the mean position. Thus, one systematic and three random displacements were calculated for each patient. Regarding the whole study cohort, the SD for the systematic error was assessed as the SD of the ten patients in the supine position or the eight patients in the prone position. The SD for the random error was taken as the SD of 30 random displacements in the supine position or 24 in the prone position for the ten or eight patients, respectively. The differences between simulation and treatment CT coordinate positions of the center of the four pelvic bony reference points along three axes were, accordingly, calculated as the axial setup errors; the SD values of systematic errors are displayed in Table 2.

Isocenter shifting model simulating systematic setup errors and prostate motion

Integration of the systematic errors of the setup and internal prostate motion

The International Commission on Radiation Units and Measurements (ICRU) report 62 discussed several scenarios about how to composite the internal margin (IM) with the setup margin (SM). The report recommended creating a "global" safety margin to be adopted by means of the quadrature formalism ($\Sigma\delta2 = IM2 + SM2$) in a quantitative approach.[19] According to the recommendation, we integrated setup errors and organ motions because the simple linear addition of two kinds of error would lead to an excessively large integrated systematic error. The calculated values of integrated systematic errors along the three axes are indicated in Table 2, for the supine and prone positions separately.

Representative shifting value of 1.65 SD along each of the three Cartesian directions

We assume that the prostate motions and setup errors can each be described by three orthogonal independent Gaussian (normal) distributions. This is a reasonable assumption, because several groups have proved that the data are nor-
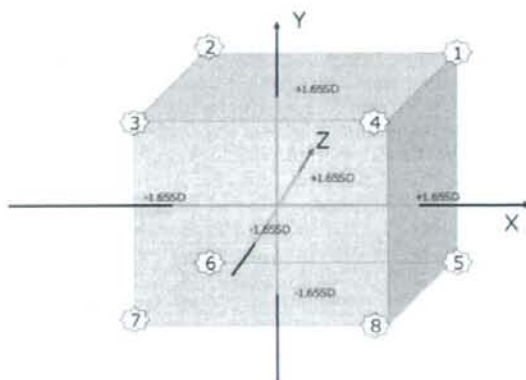

Fig. 1. Isocenter shifting model: ±1.65 SD was first chosen as the coordinate for axial check points (three pairs). Based on the six axial check points, eight vector combination points were created. The eight corner points were the worst-case scenario within a ±1.65 SD axial value

mally distributed.[4,7,10,20] In this case, the calculated integrated systematic uncertainties should also be in normal distribution. Therefore, 90% (5% to 95%) of the systematic uncertainties are included within ±1.65 SD. This is because, if we consider a patient group as a whole, the mean value of the systematic errors would be very close to zero, as indicated in our institutional results. Therefore, in this study, we chose 1.65 SD of the integrated systematic uncertainties on each of the three axes, which was expected to cover 90% of the systematic isocenter shifts in each direction.

Simulating the impacts of the systematic errors on the dose distribution

To simulate the impacts of possible large systematic errors on the dose distribution, we shifted the isocenter to the eight points with +/−1.65 SD value on each axis (vector combination points; Fig. 1).

The isocenter shifting was conducted on five IMRT plans in the prone position with hip fixation, and on five new 3D-CRT plans in the supine position without fixation, and on

the old 3D-CRT plans created using the new 3D-CRT patients' contoured images strictly complying with the protocols. To further compare the new 3D-CRT protocol with the IMRT protocol, the five new 3D-CRT plans were created based on the respective CT data set for IMRT plans in the prone position with fixation devices complying with the planning protocol accordingly. The same magnitude of systematic uncertainties in the prone position with the fixation device was applied to simulate shifting the isocenter. All the created plans were checked and were approved by our department board. Shifted plans were created and dose distributions were recalculated. In total, 160 shifted plans were created and statistical data were collected and analyzed.

Analyses based on dose volume histogram (DVH) data

With the Eclipse treatment planning system (Varian Medical Systems, Inc., Palo Alto, CA, USA), the DVHs of the PTV and the CTV (prostate) were calculated for the original plans and the total shifted plan. The total shifted plan was defined as the plan with the averaged dose distribution of the eight shifted plans for each case. Therefore, the total shifted plan was considered to be the plan reflecting the averaged effect of the simulated systematic uncertainties. For the PTV and CTV, the percentage volume covered by more than 95% of the prescription dose (V95) and the percentage prescription dose received by at least 95% volume (D95) were calculated. In addition, minimal, maximal, and mean percent doses were collected for analyses. The dose conformity to the PTV was calculated using the conformity index (CI) equation advocated by Van't Riet et al.[21] The CI is defined as the product of the fraction of the PTV receiving at least 95% of the prescription dose and the ratio of the volume of the PTV receiving at least 95% of the prescription dose to the body volume receiving at least 95% of the prescription dose, which is indicated by the following equation:

Conformity index (CI) = VPTV95%/VPTV *
                        VPTV95%/Vt.

Here, VPTV95% is the PTV volume covered by 95% of the prescription dose, VPTV is the volume of the PTV, and Vt is the body volume covered by 95% of the prescription

dose. Therefore, the CI accounts for both any normal tissue volume receiving at least 95% of the prescription dose and for any volume of the PTV receiving less than 95% of the prescription dose. For the new and old 3D-CRT plans, because the same patients' images and systematic uncertainties for simulations of isocenter shifting were applied, comparisons of the DVHs for the same PTV and CTV were made. New 3D-CRT plans created on the CT data sets in the prone position were also compared to the corresponding IMRT plans with respect to the DVH indexes. The DVHs for the shifted plan for each case were calculated using a summed plan function with the same weight assigned to each single shift. The mean DVHs both for the original and shifted plans for each protocol were calculated by averaging their corresponding percentage volume at the same incremental dose steps. The P value was calculated by the two-tailed paired Student's t-test.

Results

Table 3 and Table 4 show the planning results of the PTV and CTV for five cases using the three respective protocols. The V95 and D95 values of the CTV for the three protocols were almost comparable ($P > 0.05$) and the differences in the other indexes among the three protocols were also small. However, when the same PTV definition as for the new 3D-CRT and IMRT protocols was applied to the old 3D-CRT protocol, the V95, D95, mean dose, and CI for the old 3D-CRT cases were greatly inferior to those for the cases with the other two protocols ($P < 0.001$), indicating

Table 4. RTP results for CTV with the three protocols

	IMRT (mean ± SD)	New 3D-CRT (mean ± SD)	Old 3D-CRT (mean ± SD)
V95 (%)	100 ± 0	100 ± 0	99.9 ± 0.1
D95 (%)	100 ± 0.9	98.4 ± 0.7	97.6 ± 0.6
Minimum dose (%)	98.1 ± 1.2	97 ± 0.6	95.3 ± 1.1
Maximum dose (%)	108.3 ± 1.8	102.6 ± 0.4	101.2 ± 0.5
Mean dose (%)	103.7 ± 0.7	100.7 ± 0.7	99.6 ± 0.3

V95, Percent target volume receiving 95% of the prescription dose or higher; D95, percent prescription dose covering 95% of the target volume

Table 3. RTP results for PTV with the three protocols

	IMRT (mean ± SD)	New 3D-CRT (mean ± SD)	Old 3D-CRT (mean ± SD)
V95 (%)	99 ± 0.5	93.9 ± 0.9	59.6 ± 6.8
D95 (%)	97 ± 0.5	94.5 ± 0.3	82.9 ± 1.5
Minimum dose (%)	87.7 ± 4.8	87.5 ± 0.7	60 ± 3.3
Maximum dose (%)	108.5 ± 1.8	102.6 ± 0.4	101.3 ± 0.5
Mean dose (%)	102.3 ± 0.7	99.5 ± 0.3	94.9 ± 1
Conformity index	0.88 (0.87–0.89)	0.76 (0.72–0.78)	0.60 (0.52–0.65)

V95, Percent target volume receiving 95% of the prescription dose or higher; D95, percent prescription dose covering 95% of the target volume; conformity index = $V_{PTV95\%}/V_{PTV} * V_{PTV95\%}/Vt$ [21]
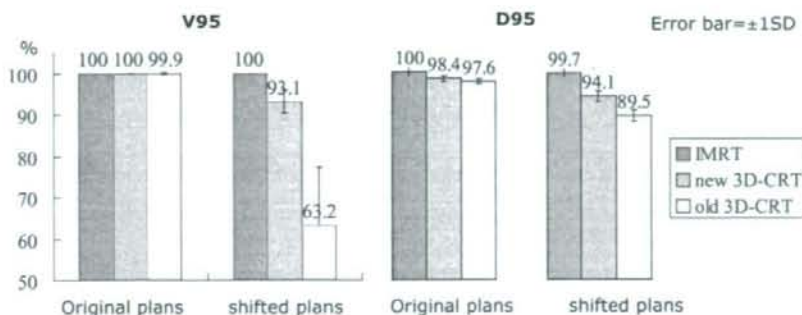For conformity index: mean (range)

V95   **D95**   Error bar=±1SD

the original MLC margins set for this protocol are insufficient if the dose evaluation is based on the current PTV concept. The CI for the IMRT plans was the highest among the three protocols, which indicates the dose distributions in the IMRT plans conform best to the PTV compared to those in the new and old 3D-CRT plans.

Figure 2 indicates the V95 and D95 of the CTV for the original plans and the simulated isocenter-shifted plans. The V95s for all three protocols were excellent and reached 100% of the prescribed dose, while D95 values were also 97% or higher for all protocols. On the other hand, although the averaged V95 for total shifted IMRT plans was maintained at 100%, those for the new 3D-CRT and old 3D-CRT plans decreased to 93.1% and 63.2%, respectively. The decreasing rate of the V95 values for the old 3D-CRT cases was most evident compared with those for the other two protocol's cases. The same trend as for V95 was observed with respect to D95, although the magnitudes of the deterioration after simulating the systematic uncertainties in the old 3D-CRT cases were relatively smaller than those for the V95. The net decrease for IMRT cases was minimum (0.3%), while that for the old 3D-CRT cases was the biggest (8.1%) among the three protocols.

Figure 3 indicates the mean DVHs of the CTV for the original and total shifted plans of the three protocols. For the IMRT protocol, the two curves almost coincided with each other. Compared with the original new 3D-CRT plans, definitive insufficient dose coverage was observed with respect to the total shifted plans. Again here, the worsening of the CTV dose coverage for the old 3D-CRT plans was the most marked among the protocols. The detailed net decreases in the DVH statistics of the CTV after simulating the systematic uncertainties are indicated in Table 5.

The mean DVH of the CTV for the new 3D-CRT plans created on the CT data sets for the IMRT protocol is shown in Fig. 4. The net decreases in the V95, D95, minimum dose, maximum dose, and the mean dose for the IMRT protocol, the new 3D-CRT protocol, and the new 3D-CRT plans created on the CT data sets scanned in the prone position are indicated in Fig. 5. Although the net decreases in the V95, D95, minimum dose, maximum dose, and mean dose became much smaller when the new 3D-CRT plans were created with the patients in the prone position with hip fixation than when created with the patients in the supine
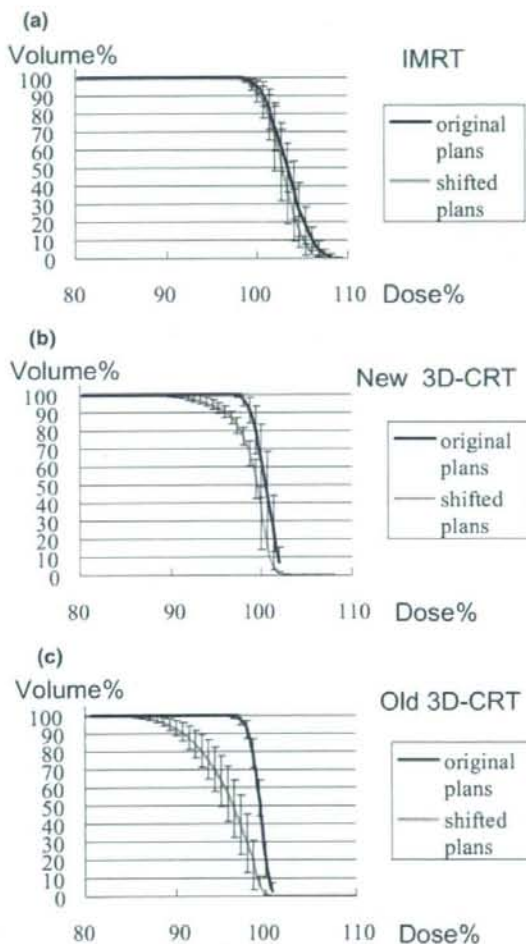
(a)

(b)

(c)

Fig. 3a–c. Mean DVH of the CTV before and after taking systematic uncertainties into consideration, for IMRT (a), new 3D-CRT (b), and old 3D-CRT protocols (c). *Error bar*, ±1 SD

Table 5. Comparison of the net decreases in the DVH statistics of the CTV for the three protocols after simulation of systematic uncertainties

	IMRT		New 3D-CRT		Old 3D-CRT	
	Net decrease (%)	P value	Net decrease (%)	P value	Net decrease (%)	P value
V95	0	0.4	6.9	0.005	36.7	0.004
D95	0.3	0.02	4.3	0.001	8.1	<0.0001
Min.	2.4	0.1	8.3	0.0001	11.8	<0.0001
Max.	1.7	0.003	1	0.006	1.3	0.003
Mean	0.7	<0.0001	1.5	0.0007	3.7	0.0008

V95, Percent target volume receiving 95% of the prescription dose or higher; D95, percent prescription dose covering 95% of the target volume
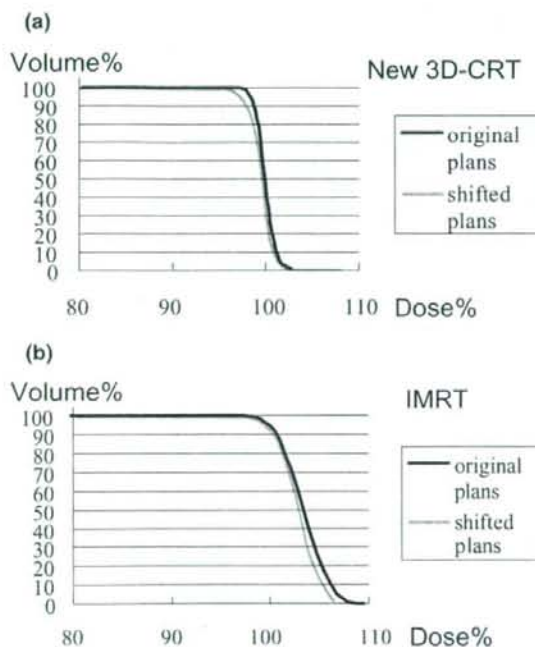

(a)

Volume%

New 3D-CRT

original plans

shifted plans

(b)

Volume%

IMRT

original plans

shifted plans

Fig. 4a,b. Comparison of the mean DVH of the CTV, for the new 3D-CRT (**a**) and IMRT plans (**b**) before and after taking systematic uncertainties into consideration based on the same condition: new 3D-CRT plans were created on the IMRT plan images and the systematic uncertainties of the prone position with hip fixation were simulated for the two protocol plans

position without fixation, the IMRT plans still had some advantages in terms of target coverage.

Discussion

The ICRU report 50[22] recommends defining a geometrical structure of PTV to compensate for the effect of uncertainties. The magnitude of PTV can predict and project the potential location of the CTV. Margins to create the PTV
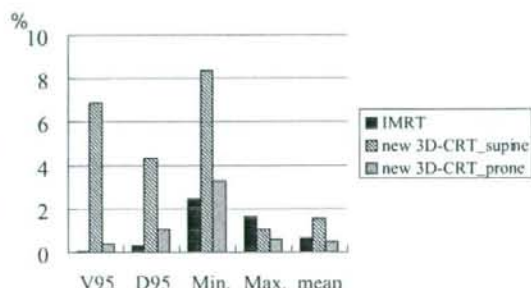

Fig. 5. Net decrease in the DVH indexes of the CTV for IMRT, new 3D-CRT_supine, and new 3D-CRT_prone plans after taking systematic uncertainties into consideration. *New 3D-CRT_supine* represents the new 3D-CRT plans simulating the systematic uncertainties in the supine position without using an immobilization device. *New 3D-CRT_prone* represents the new 3D-CRT plans created based on the IMRT plan images simulating the systematic uncertainties in the prone position with hip fixation

from the CTV (PTV margin) should take into account both setup errors and internal organ motion. However, in most cases, the CTV is often located adjacent to the organs at risk (OARs), which prevents us from using margins large enough to cover all of the uncertainties for most patients. Therefore, adequate margins to compensate for 90%–95% of the uncertainties should be used to create the PTV. More importantly, the magnitude of the adequate margin is also influenced by the method of patient fixation or error reduction strategies. To see whether the defined margins account for the uncertainties, we examined and compared the adequacy of three definitive radiotherapy protocols for localized prostate cancer, in terms of the CTV coverage, by simulating possible large systematic errors with respect to patient setup and internal organ motion.

In the present study, several assumptions were made, based on the previously published literature; we assumed that random errors have a relatively smaller impact on the dose distribution to the prostate,[15-17] while systematic errors are in normal distribution.[4,7,10,20] Because our purpose was to compare planning strategies of three different radiotherapy protocols and to estimate their validity by verifying the tolerability in CTV coverage, we only simulated systematic

errors. To include all the possible systematic uncertainties, it would be necessary to apply nearly ±3 SD. However, we carefully chose ±1.65 SD of the systematic error as a check-point value for the isocenter shift, which includes 90% (from 5% to 95%) systematic uncertainties along each axis. Therefore, there were in total eight check points (Fig. 1). With these check points, we expected to include most of the possible systematic displacements while excluding very extreme shifts, which is reasonable for comparing the adequacy among different radiotherapy protocols.

Our previous study showed that the dynamic-arc 3D-CRT (new 3D-CRT) could achieve a comparable dose distribution to that achieved with IMRT with respect to the target coverage and rectal sparing in external-beam radiotheapy for localized prostate cancer with a prescription dose of 74 Gy. On the other hand, the old 3D-CRT plan could not reach a qualified dose coverage for the target, based on the current PTV concept, due to the universally smaller portal margins applied.[18] This continuing study shows that when the systematic uncertainties were incorporated into the dose distribution analyses, the difference between the planned and the actually delivered target dose was much larger for the old 3D-CRT plan, and a detectable dose decrease also appeared in the dynamic-arc 3D-CRT plan. However, the IMRT plan still maintained an intended target coverage of the prostate (CTV). Therefore the IMRT protocol is considered to be superior to the dynamic-arc 3D-CRT plan in terms of tolerability against systematic uncertainties.

A big question here is what are the adequate acceptance criteria with respect to the dose decrease from the planned to the actually delivered dose supposing the random factors could be neglected. The answer could not be drawn from the literature. van Herk[17] discussed this point in his review article and analyzed several examples, but the criteria were diverse and could not be uniformly applied: they should be institution-dependent and also treatment-technique-dependent. A general guideline for the target coverage in traditional static dose distribution is reported in ICRU report 50,[22] where the PTV should guarantee that 95% of the prescription dose is delivered to at least 90% of the CTV. Based on this guideline, the actually delivered dose distribution with the old 3D-CRT plans is unacceptable, which means margins applied directly to the CTV and simply defined by jaws/MLCs are universally insufficient to account for systematic uncertainties. However, the difference between the planned and actually delivered dose distribution to the CTV with IMRT plans is nominal, indicating that the margins set successfully compensate for the systematic uncertainties.

There are two main reasons why the ability to account for the systematic uncertainties between our IMRT and the new 3D-CRT protocol plans is different. One is patient position-related and immobilization-related uncertainty values, and the other is the treatment techniques themselves, which define dose conformity to, and the dose gradient from, the PTV. A comparison of the effect of the systematic uncertainties on the new 3D-CRT plans and the IMRT plans based on the same image pool simulating the same values of uncertainties, resulted in the slight supe-riority of the IMRT protocol to the new 3D-CRT protocol to account for the systematic uncertainties. At the same time, we also noticed that the degree of decrease in dose coverage after simulating the systematic uncertainties for the new 3D-CRT plans was much smaller when the patients were fixed in the prone position and immobilized with hip fixation than when they were treated in the supine position without any fixation devices. This may indicate that if, for our new 3D-CRT protocol, we also immobilize patients in the prone position with hip fixation, as is done with the patients receiving the IMRT protocol, we may get much better actual dose distribution. It has been reported that the prostate movement in the prone position was much larger that that in the supine position if no fixation devices were used, probably because of the effect of respiration.[11] Therefore, it is strongly recommended that we should use a fixation device when treating patients in the prone position.

There were some remarks in the literature that the IMRT was more sensitive to uncertainties than 3D-CRT due to its sharper dose gradients in the peripheral region of the PTV. Our data show that this is not necessarily true. The sensitivity to treatment-related uncertainties strongly depends on the given margins for the PTV and the error reduction strategies applied, as well as the degree of dose fall-off outside the PTV.

One drawback of the present study was that the effect of systematic uncertainties on the doses to the rectum and bladder was not incorporated into the dose distribution analyses of the target. The original planned dose range to the rectum and bladder was large, and rectum filling was diverse; all these factors make the incorporation much more complicated. Therefore, we believe a deformable image registration technique should be incorporated in the treatment planning based on a 4D imaging data set in the future.

In conclusion, differences in the CTV dose among three protocols for definitive external-beam radiotherapy when systematic uncertainties were taken into consideration were evaluated. Our current IMRT protocol, with fixation devices used in the prone position, was considered to successfully compensate for decreased systematic uncertainties, while the old 3D-CRT protocol was inadequate to realize an adequate CTV dose, although the CTV dose was sufficient in terms of the static protocol data. In the future, a 4D dataset-based method for radiotherapy protocol evaluation will be necessary to accurately estimate the actually delivered dose to the targets and organs at risk.

References

1. Bijhold J, Lebesque JV, Hart AA, et al. (1992) Maximizing setup accuracy using portal images as applied to a conformal boost technique for prostatic cancer. Radiother Oncol 24:261–271

2. Hurkmans CW, Remeijer P, Lebesque JV, et al. (2001) Setup verification using portal imaging; review of current clinical practice. Radiother Oncol 58:105–120

3. Vigneault E, Pouliot J, Laverdiere J, et al. (1997) Electronic portal imaging device detection of radioopaque markers for the evaluation of prostate position during megavoltage irradiation: a clinical study. Int J Radiat Oncol Biol Phys 37:205–212

4. Antolak JA, Rosen II, Childress CH, et al. (1998) Prostate target volume variations during a course of radiotherapy. Int J Radiat Oncol Biol Phys 42:661–672

5. Beard CJ, Kijewski P, Bussiere M, et al. (1996) Analysis of prostate and seminal vesicle motion: implications for treatment planning. Int J Radiat Oncol Biol Phys 34:451–458

6. Lattanzi J, McNeely S, Hanlon A, et al. (1998) Daily CT localization for correcting portal errors in the treatment of prostate cancer. Int J Radiat Oncol Biol Phys 41:1079–1086

7. Roeske JC, Forman JD, Mesina CF, et al. (1995) Evaluation of changes in the size and location of the prostate, seminal vesicles, bladder, and rectum during a course of external beam radiation therapy. Int J Radiat Oncol Biol Phys 33:1321–1329

8. Stroom JC, Koper PC, Korevaar GA, et al. (1999) Internal organ motion in prostate cancer patients treated in prone and supine treatment position. Radiother Oncol 51:237–248

9. Zelefsky MJ, Crean D, Mageras GS, et al. (1999) Quantification and predictors of prostate position variability in 50 patients evaluated with multiple CT scans during conformal radiotherapy. Radiother Oncol 50:225–234

10. Balter JM, Sandler HM, Lam K, et al. (1995) Measurement of prostate movement over the course of routine radiotherapy using implanted markers. Int J Radiat Oncol Biol Phys 31:113–118

11. Kitamura K, Shirato H, Seppenwoolde Y, et al. (2002) Three-dimensional intrafractional movement of prostate measured during real-time tumor-tracking radiotherapy in supine and prone treatment positions. Int J Radiat Oncol Biol Phys 53:1117–1123

12. Wu J, Haycocks T, Alasti H, et al. (2001) Positioning errors and prostate motion during conformal prostate radiotherapy using on-line isocentre setup verification and implanted prostate markers. Radiother Oncol 61:127–133

13. Little DJ, Dong L, Levy LB, et al. (2003) Use of portal images and BAT ultrasonography to measure setup error and organ motion for prostate IMRT: implications for treatment margins. Int J Radiat Oncol Biol Phys 56:1218–1224

14. Trichter F, Ennis RD (2003) Prostate localization using transabdominal ultrasound imaging. Int J Radiat Oncol Biol Phys 56: 1225–1233

15. Bortfeld T, Jiang SB, Rietzel E (2004) Effects of motion on the total dose distribution. Semin Radiat Oncol 14:41–51

16. Levitt SH, Khan FM (2001) The rush to judgment: does the evidence support the enthusiasm over three-dimensional conformal radiation therapy and dose escalation in the treatment of prostate cancer? Int J Radiat Oncol Biol Phys 51:871–879

17. van Herk M (2004) Errors and margins in radiotherapy. Semin Radiat Oncol 14:52–64

18. Zhu S, Mizowaki T, Nagata Y, et al. (2005) Comparison of three radiotherapy treatment planning protocols of definitive external-beam radiation for localized prostate cancer. Int J Clin Oncol 10:398–404

19. International Commission on Radiation Units and Measurements (1999) ICRU Report 62: prescribing, recording, and reporting photon beam therapy (supplement to ICRU report 50). Oxford University Press, Oxford

20. Rudat V, Schraube P, Oetzel D, et al. (1996) Combined error of patient positioning variability and prostate motion uncertainty in 3D conformal radiotherapy of localized prostate cancer. Int J Radiat Oncol Biol Phys 35:1027–1034

21. van't Riet A, Mak AC, Moerland MA, et al. (1997) A conformation number to quantify the degree of conformality in brachytherapy and external beam irradiation: application to the prostate. Int J Radiat Oncol Biol Phys 37:731–736

22. International Commission on Radiation Units and Measunements (1993) ICRU Report 50: prescribing, recording, and reporting photon beam therapy. Oxford University Press, Oxford

CLINICAL INVESTIGATION

Radiation Oncology Practice

JAPANESE STRUCTURE SURVEY OF RADIATION ONCOLOGY IN 2005 BASED ON INSTITUTIONAL STRATIFICATION OF PATTERNS OF CARE STUDY

Teruki Teshima, M.D.,* Hodaka Numasaki, M.S.,* Hitoshi Shibuya, M.D.,[†]
Masamichi Nishio, M.D.,[‡] Hiroshi Ikeda, M.D.,[§] Hisao Ito, M.D.,[¶] Kenji Sekiguchi, M.D.,[‖]
Norihiko Kamikonya, M.D.,[#] Masahiko Koizumi, M.D.,** Masao Tago, M.D.,[††]
Yasushi Nagata, M.D.,[‡‡] Hidekazu Masaki, M.D.,[§§] Tetsuo Nishimura, M.D.,[¶¶]
Shogo Yamada, M.D.,[‖‖] and Japanese Society of Therapeutic Radiology and
Oncology Database Committee

*Department of Medical Physics and Engineering, Osaka University Graduate School of Medicine, Suita, Osaka, Japan; [†]Department of Radiology, Tokyo Dental and Medical University, Tokyo, Japan; [‡]Department of Radiology, National Hospital Organization Hokkaido Cancer Center, Sapporo, Hokkaido, Japan; [§]Division of Radiation Oncology, National Cancer Center, Tokyo, Japan; [¶]Department of Radiology, Chiba University Graduate School of Medicine, Chiba, Japan; [‖]Department of Radiation Oncology, St. Luke's International Hospital, Tokyo, Japan; [#]Department of Radiology, Hyogo College of Medicine, Nishinomiya, Hyogo, Japan; **Department of Radiological Technology, Fujita Health University School of Health Sciences, Nagoya, Aichi, Japan; [††]Department of Radiology, University of Tokyo Hospital, Tokyo, Japan; [‡‡]Department of Radiation Oncology and Image-Applied Therapy, Kyoto University Graduate School of Medicine, Kyoto, Japan; [§§]Department of Radiology, National Center for Child Health and Development, Tokyo, Japan; [¶¶]Division of Radiation Oncology, Shizuoka Cancer Center, Shizuoka, Japan; and [‖‖]Tohoku University Hospital Cancer Center, Sendai, Japan

Purpose: To evaluate the structure of radiation oncology in Japan in terms of equipment, personnel, patient load, and geographic distribution to identify and improve any deficiencies.
Methods and Materials: A questionnaire-based national structure survey was conducted between March 2006 and February 2007 by the Japanese Society of Therapeutic Radiology and Oncology. These data were analyzed in terms of the institutional stratification of the Patterns of Care Study.
Results: The total numbers of new cancer patients and total cancer patients (new and repeat) treated with radiotherapy in 2005 were estimated at approximately 162,000 and 198,000, respectively. In actual use were 765 linear accelerators, 11 telecobalt machines, 48 GammaKnife machines, 64 ^{60}Co remote-controlled after-loading systems, and 119 ^{192}Ir remote-controlled after-loading systems. The linear accelerator systems used dual-energy function in 498 systems (65%), three-dimensional conformal radiotherapy in 462 (60%), and intensity-modulated radiotherapy in 170 (22%). There were 426 Japanese Society of Therapeutic Radiology and Oncology-certified radiation oncologists, 774 full-time equivalent radiation oncologists, 117 medical physicists, and 1,635 radiation therapists. Geographically, a significant variation was found in the use of radiotherapy, from 0.9 to 2.1 patients/1,000 population. The annual patient load/FTE radiation oncologist was 247, exceeding the Blue Book guidelines level. Patterns of Care Study stratification can clearly discriminate the maturity of structures according to their academic nature and caseload.
Conclusions: The Japanese structure has clearly improved during the past 15 years in terms of equipment and its use, although the shortage of manpower and variations in maturity disclosed by this Patterns of Care Study stratification remain problematic. These constitute the targets for nationwide improvement in quality assurance and quality control. © 2008 Elsevier Inc.

Structure survey, Radiotherapy facility, Radiotherapy personnel, Radiotherapy equipment, Caseload.

INTRODUCTION

The medical care systems of the United States and Japan have very different backgrounds. In 1990, the Patterns of Care Study (PCS) conducted a survey of the 1989 structure of radiation oncology facilities for the entire census of facilities in the United States. The results of the survey, together with trends in the structure of specialization since 1974, were reported in detail by Owen *et al.* (1). In 1991, the Japanese Society of Therapeutic Radiation Oncology (JASTRO) conducted the first national survey of the structure of radiotherapy (RT) facilities in Japan based on their status in 1990, with the results reported by Tsunemoto (2). The first comparison of these two national structure surveys to illustrate the similarities and differences present in 1989–1990 was conducted by Teshima *et al.* (3) and reported in 1995. The resultant international exchange of information proved valuable for both countries, because each could improve their own structure of radiation oncology using those data.

The Japanese structure of radiation oncology has improved in terms of the greater number of cancer patients who are treated with RT, as well as the public awareness of the importance of RT, although problems still exist that should be solved. The JASTRO has conducted national structure surveys every 2 years since 1990 (4). In Japan, an anticancer law was enacted in 2006 in response to patients' urgent petitions to the government. This law strongly advocates the promotion of RT and increasing the number of radiation oncologists (ROs) and medical physicists. The findings of the international comparisons and the consecutive structural data gathered and published by the JASTRO have been useful in convincing the Japanese bureaucracy of the importance of RT. In this report, the recent structure of radiation oncology in Japan is presented, with reference to data obtained from previous international comparisons.

METHODS AND MATERIALS

Between March 2006 and February 2007, the JASTRO conducted a questionnaire using a national structure survey of radiation oncology in 2005. The questionnaire included the number of treatment machines by type, number of personnel by category, and number of patients by type, site, and treatment modality. For variables measured over a period, data were requested for the calendar year

2005. The response rate was 712 (96.9%) of 735 of active facilities. The data from 511 institutions (69.5%) were registered in the International Directory of Radiotherapy Centres in Vienna, Austria in April 2007.

The PCS was introduced in Japan in 1996 (5–11). The PCS in the United States used structural stratification to analyze the national averages for the data in each survey item using two-stage cluster sampling. The Japanese PCS used similar methods. We stratified the RT facilities nationwide into four categories for the regular structure surveys. This stratification was based on academic conditions and the annual number of patients treated with RT in each institution, because the academic institutions require, and have access to, more resources for education and training and the annual caseload also constitutes essential information related to structure. For the present study, the following institutional stratification was used: A1, university hospitals/cancer centers treating ≥440 patients/y; A2, the same type of institutions treating ≤439 patients/y; B1, other national/public hospitals treating ≥130 patients/y; and B2, other national hospital/public hospitals treating ≤129 patients/y.

The Statistical Analysis Systems, version 8.02 (SAS Institute, Cary, NC), software program (12) was used for statistical analyses, and statistical significance was tested using the chi-square test, Student t test, or analysis of variance.

RESULTS

Current situation of radiation oncology in Japan

Table 1 shows that the numbers of new patients and total patients (new plus repeat) requiring RT in 2005 were estimated at approximately 162,000 and 198,000, respectively. According to the PCS stratification of institutions, almost 40% of the patients were treated at academic institutions (categories A1 and A2), even though these academic institutions constituted only 18% of the 732 RT facilities nationwide.

The cancer incidence in Japan in 2005 was estimated at 660,578 (13) with approximately 25% of all newly diagnosed patients treated with RT. The number has increased steadily during the past 10 years and is predicted to increase further (4).

Facility and equipment patterns

Table 2 lists the RT equipment and related function. In actual use were 767 linear accelerators, 11 telecobalt machines, 48 Gamma Knife machines, 65 ^{60}Co remote-controlled afterloading systems (RALSs), and 119 ^{192}Ir RALSs. The linear accelerator system used dual-energy function in 498 systems

Table 1. PCS stratification of radiotherapy facilities in Japan

Institution Category	Description	Facilities (*n*)	New patients (*n*)	Average new patients/facility* (*n*)	Total patients (new + repeat) (*n*)	Average total patients/facility* (*n*)
A1	UH and CC (≥440 patients/y)	66	45,866	694.9	54,885	831.6
A2	UH and CC (<440 patients/y)	67	17,161	256.1	21,415	319.6
B1	Other (≥130 patients/y)	290	71,627	247.0	88,757	306.1
B2	Other (<130 patients/y)	289	21,664	75.0	26,116	90.4
Total		712	156,318†	219.5	191,173†	268.5

Abbreviations: PCS = Patterns of Care Study; UH = university hospital; CC = cancer center hospital; Other = other national, city, or public hospital.

* $p < 0.0001$.

† Number of radiotherapy institutions was 735 in 2005, and number of new patients was estimated at approximately 162,000; corresponding number of total patients (new plus repeat) was 198,000.

Table 2. Equipment, its function and patient load per equipment by PCS institutional stratification

RT equipment and function	A1 (n = 66)		A2 (n = 67)		B1 (n = 290)		B2 (n = 289)			Total (n = 712)	
	n	%	n	%	n	%	n	%	p	n	%
Linear accelerator	133		85		283		264		—	765	
With dual energy function	97	72.9*	62	72.9*	197	69.6*	142	53.8*	<0.0001	498	65.1*
With 3D-CRT function (MLC width ≤1.0 cm)	109	82.0*	59	69.4*	176	62.2*	118	44.7*	<0.0001	462	60.4*
With IMRT function	65	48.9*	25	29.4*	55	19.4*	25	9.5*	<0.0001	170	22.2*
Annual patients/linear accelerator	412.7†		243.8†		279.9†		93.4†		<0.0001	234.6†	
Particle	5		0		1		1		—	7	
Tomotherapy			0		0		1		—	1	
Microtron	8		3		9		4		—	24	
Telecobalt (actual use)	7 (5)		6 (1)		7 (1)		14 (4)		—	34 (11)	
Gamma Knife	6		3		32		7		0.0004	48	
^{60}Co RALS (actual use)	8 (8)	12.1‡ (12.1)	13 (12)	19.4‡ (17.9)	41 (36)	14.1‡ (12.4)	12 (8)	4.2‡ (2.8)	<0.0001	74 (64)	10.4‡ (9.0)
^{192}Ir RALS (actual use)	53 (52)	80.3‡ (78.8)	27 (24)	38.8‡ (34.3)	35 (35)	12.1‡ (12.1)	8 (8)	2.8‡ (2.8)	<0.0001	123 (119)	17.1‡ (16.6)
^{137}Cs RALS (actual use)	0 (0)		0 (0)		2 (2)		0 (0)		—	2 (2)	

Abbreviations: PCS = Patterns of Care Study; RT = radiotherapy; 3D-CRT = three-dimensional conformal radiotherapy; MLC = multileaf collimator; IMRT = intensity-modulated radiotherapy; RALS = remote-controlled after-loading system.

* Percentage calculated from number of systems using this function and total number of linear accelerator systems.

† Percentage calculated from number patients and number of institutions with linear accelerators; institutions without linear accelerators excluded from calculation.

‡ Percentage of institutions that have this equipment (≥2 pieces of equipment per institution).

(65%), three-dimensional conformal RT in 462 (60%), and intensity-modulated RT (IMRT) in 170 (22%). These functions were installed more frequently in the equipment of academic institutions than in that of nonacademic institutions ($p <$ 0.0001). The annual numbers of patients/linear accelerator were 413 for A1, 244 for A2, 280 for B1, and 93 for B2 institutions. The number of institutions with telecobalt machines in actual use showed a major decrease to 11. The Gamma-Knife machine was installed more frequently in B1 institutions. A significant replacement of ^{60}Co RALS by ^{192}Ir RALS was observed, especially in academic institutions. We had seven particle machines, three with carbon beam and five with proton beam RT. The total number of patients treated at the seven institutions was estimated at approximately 1,600 (1% of all new patients in Japan). Eleven advanced institutions were included in the A1 category and treated >800 patients annually. They were equipped with linear accelerators with dual-energy function (71% of the institutions), three-dimensional conformal RT function (89%) and IMRT function (70%), as well as with ^{192}Ir-RALS (90%) and a computed tomography (CT) simulator (100%).

Table 3 lists the RT planning and other equipment. X-ray simulators were installed in 70% of all institutions, and CT simulators in 55%. A significant difference was found in the rate of CT simulator installation by institutional stratification, from 91% in A1 to 45% in B2 institutions ($p < 0.0001$). Only a very few institutions used magnetic resonance imaging for RT, although computer use for RT recording was pervasive.

Staffing patterns and patient loads

Table 4 lists the staffing patterns and patients loads by institutional stratification. The total number of full-time equivalent (FTE) ROs in Japan was 774. The average number of FTE ROs was 4.41 for A1, 1.43 for A2, 0.89 for B1, and 0.45 for B2 institutions ($p < 0.0001$). The patient load/FTE RO in Japan was 247, and the number for A1, A2, B1, and B2 institutions was 189, 224, 343, and 202, respectively ($p < 0.0001$), with the patient load for B1 institutions by far the greatest. In Japan, 40% of the institutions providing RT had their own designated beds, and ROs must also take care of their inpatients. The percentage of distribution of institutions by patient load/FTE RO is shown in Fig. 1 and indicates that the largest number of facilities featured a patient/FTE staff level of 101–150, with 151–200 the second largest number. More than 60% of the institutions (438 of 712) had <1 FTE RO, as shown by the gray areas of the bars.

A similar trend for radiation technologists and their patient load by stratification of institutions was observed ($p <$ 0.0001). The percentage of distribution of institutions by patient load/radiation technologist is also shown in Fig. 2. The largest number of facilities had a patient/RT technologist level in the 81–100 range, with 101–120 the second largest number. There were 117 full-time (and 30 part-time) medical physicists and 257 full-time (and 13 part-time) RT quality assurance staff. In this survey, duplication reporting of these personnel numbers could not be checked because of a lack of

Table 3. Radiotherapy planning and other equipments by PCS institutional stratification

RT planning and other equipment	A1 (n = 66)		A2 (n = 67)		B1 (n = 290)		B2 (n = 289)		Total (n = 712)		
	n	%	n	%	n	%	n	%	n	%	p
X-ray simulator	58	84.8*	53	76.1*	201	68.6*	190	65.7*	502	69.7*	0.0130
CT stimulator	66	90.9*	48	68.7*	163	54.8*	130	44.6*	407	55.3*	<0.0001
RTP computer (≥2)	209 (190)	100* (71.2)	114 (82)	94.0* (46.3)	336 (101)	95.9 (14.8)	281 (50)	88.6* (8.7)	940 (146)	93.1* (20.5)	0.0005 (<0.0001)
MRI (≥2)	164 (153)	95.5* (78.8)	134 (124)	94.0* (79.1)	470 (351)	96.9 (55.9)	344 (148)	92.4* (24.6)	1,112 (338)	94.7* (47.5)	0.1136 (<0.0001)
For RT only	3	3.0*	1	1.5*	5	1.7*	3	0.7*	12	1.4*	
Computer use for RT recording	63	95.5*	62	92.5*	263	90.7*	238	82.4*	626	87.9*	0.0015

Abbreviations: CT = computed tomography; RTP = radiotherapy planning; MRI = magnetic resonance imaging; other abbreviations as in Table 2.

* Percentage of institutions that have equipment (≥2 pieces of equipment per institution).

individual identification on staffing data. Finally, there were 907 nurses and clerks.

Distributions of primary sites, specific treatment and palliative treatment

Table 5 lists the distribution of primary sites by institutional stratification. The most common disease site was the breast, followed by lung/bronchus/mediastinum and genitourinary. In Japan, the number of patients with prostate cancer undergoing RT was approximately 13,200 in 2005, but the number has been increasing most rapidly. The stratification of institutions indicated that more patients with lung cancer were treated at the nonacademic institutions (B1 and B2), and more patients with head-and-neck cancer were treated at academic institutions (A1 and A2; $p < 0.0001$).

Table 6 lists the distribution of use of specific treatment and the number of patients treated with these modalities by the PCS stratification of institutions. Brachytherapy, such as intracavitary RT, interstitial RT, and radioactive iodine therapy, for prostate cancer was used more frequently in academic institutions than in nonacademic institutions ($p < 0.0001$). Similar trends were observed for other specific treatments such as total body RT, intraoperative RT, stereotactic brain RT, stereotactic body RT, IMRT, thermoradiotherapy, and RT of the pterygium by ^{90}Sr. In 2005, 4.6% of patients ($n = 755$) were treated with IMRT at 33 institutions. This percentage was significantly lower than that of institutions using linear accelerators with IMRT function (22%; Table 2).

Table 7 lists the number of patients with any type of brain metastasis or bone metastasis treated with RT according to the same institutional stratification. B1 institutions treated more patients with brain metastasis (11% of all patients) than other types of institutions ($p < 0.0001$), and the use of RT for bone metastasis ranged from 11% for A1 to 19% for B2 ($p < 0.0001$). Overall, more patients were treated with RT at nonacademic type B2 institutions than at A1 or A2 institutions.

Geographic patterns

Figure 3 shows the geographic distributions of the annual number of patients (new plus repeat) per 1,000 population by 47 prefectures arranged in order of increasing number of JASTRO-certified physicians per 1,000,000 population (14). Significant differences were found in the use of RT, from 0.9 patients/1,000 population (Saitama and Okinawa) to 2.1 (Hokkaido). The average number of patients/1,000 population per quarter ranged from 1.37 to 1.57 ($p = 0.2796$). A tendency was found for a greater number of JASTRO-certified physicians to be accompanied by an increased use of RT for cancer patients, although the correlation was not statistically significant. The use rate of RT in a given prefecture was not necessarily related to its population density in 2005, just as we observed in the 1990 data (3).

DISCUSSION

In 1990, fewer facilities for RT were available and fewer patients were treated with RT in Japan than in the United States. However, the numbers for Japan improved

Table 4. Structure and personnel by PCS institutional stratification

|	Structure and personnel					
	A1 (n = 66)	A2 (n = 67)	B1 (n = 290)	B2 (n = 289)	p-value	Total (n = 712)
Institutions/total institutions (%)	9.3	9.4	40.7	40.6		100
Institutions with RT bed (n)	57 (86.4)	35 (52.2)	127 (43.8)	68 (23.5)		287 (40.3)
Average RT beds/institution (n)	14.0	4.8	3.4	1.0		3.6
JASTRO-certified RO (full time)	181	62	139	44		426
Average JASTRO-certified RO/institution (n)	2.7	0.9	0.5	0.2	<0.0001	0.6
Total (full-time and part-time) RO FTE*	290.9	95.55	258.77	129.24		774.46
Average FTE ROs/institution	4.41	1.43	0.89	0.45	<0.0001	1.09
Patient load/FTE RO	188.7	224.1	343.0	202.1	<0.0001	246.8
Total RT* technologists	388.6	176.3	637.7	431.9		1634.5
Average technologists/institution (n)	5.9	2.6	2.2	1.5	<0.0001	2.3
Patient load/RT technologist	141.2	121.5	139.2	60.5	<0.0001	117.0
Total nurses/assistants/clerks (n)	202.2	92.4	390.55	221.8		907
Full-time medical physicists + part-time (n)	51 + 10.1	8 + 7	39 + 7	19 + 6		117 + 30.1
Full-time RT QA staff + part-time	81 + 0	31 + 7	102.5 + 3	42.3 + 3		256.8 + 13

Abbreviations: JASTRO = Japanese Society of Therapeutic Radiation Oncology; RO = radiation oncologist; FTE = full-time equivalent (40 h/wk only for RT practice); QA = quality assurance; other abbreviations as in Table 2.

Data in parentheses are percentages.

significantly during the next 15 years, with respective increases by factors of 2 and 2.6 compared with those in 1990 (3). However, the use rate of RT for new cancer patients remained at 25%, less than one-half the ratio in the United States and European countries. The anticancer law was enacted in Japan to promote RT and education for ROs, as well as medical physicists or other staff members, from April 2006. For the implementation of this law, comparative data of the structure of radiation oncology in Japan and the United States, as well as relevant PCS data, proved helpful. Because

the increase in the elderly population of developed countries is the greatest in Japan, RT is expected to play an increasingly important role.

Compared with 1990, the number of linear accelerator systems increased significantly by 2.3 times, and the percentage of systems using telecobalt decreased to 7%. Furthermore, the functions of linear accelerators, such as dual energy, three-dimensional conformal RT (multileaf collimator width <1 cm), and IMRT improved. The number of high-dose-rate RALS in use increased by 1.4 times and the use of
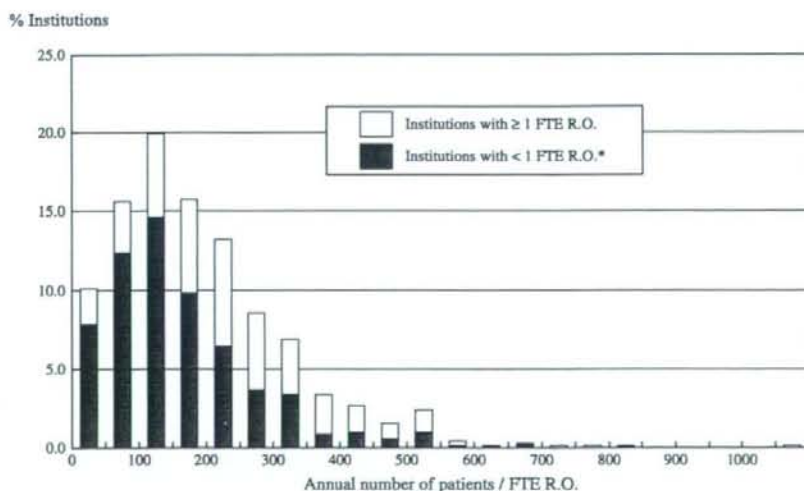
% Institutions

* Number of .FTEs for institutions with FTE<1 was calculated as FTE=1 to avoid overestimating pateint' load/R.O.

Fig. 1. Percentage of institutions by patient load/full-time equivalent (FTE) staff of radiation oncologists (RO) in Japan. White bars represent institutions with one or more FTE staff, and gray bars represent institutions with fewer than one FTE radiation oncologist. Each bar represents interval of 50 patients/FTE radiation oncologist.
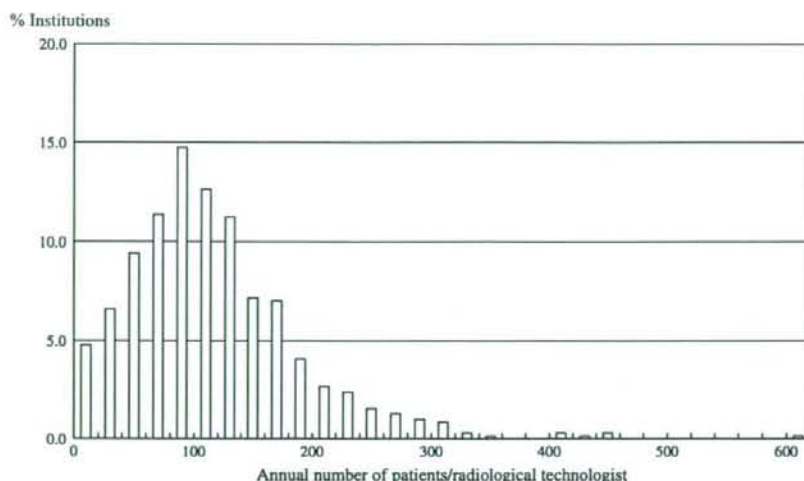
% Institutions

Fig. 2. Percentage of institutions by patient load/radiotherapy technologist in Japan. Each bar represents interval of 20 patients/full-time equivalent staff.

^{60}Co-RALS has largely been replaced by ^{192}Ir-RALS. CT simulators were installed in 55% of institutions nationwide, and RT planning systems were used in 93%, for an increase in the number of RT planning systems of 4.87 times. The maturity of the functions of linear accelerator and greater possession rates of CT simulators and systems using ^{192}Ir-RALS were closely related to the institutional stratification by PCS, which could therefore aid in the accurate discrimination of structural maturity and immaturity and the identification of structural targets to be improved. The Japanese PCS group published structural guidelines based on the PCS data (16), and we plan to use this structural data for a new PCS to revise the Japanese structural guidelines.

The staffing patterns in Japan also improved in terms of numbers. However, the institutions that had fewer than one FTE RO on their staff still accounted for >60% nationwide, and this rate did not change during the 15 years from 1990 to 2005. In Japan, most institutions still rely on part-time ROs. First, the number of cancer patients who require RT is increasing more rapidly than the number of ROs. Second, specialist fees for ROs in academic institutions are not recognized by the Japanese medical care insurance system, which is strictly controlled by the government. Most ROs must therefore work part-time at affiliated hospitals in the B1 and B2 groups to earn a living. Thus, to reduce the number of institutions that rely on part-time ROs and might encounter

Table 5. Primary sites of cancer treatment with RT in 2005 by PCS institutional stratification for new patients

Primary site	A1 ($n = 65$)		A2 ($n = 67$)		B1 ($n = 285$)		B2 ($n = 284$)		Total ($n = 701$)	
	n	%	n	%	n	%	n	%	n	%
Cerebrospinal	2,603	5.6	770	4.5	4,431	6.4	795	3.6	8,599	5.6
Head and neck (including thyroid)	6,318	13.7	2,372	13.9	6,033	8.7	1,650	7.5	16,373	10.6
Esophagus	3,164	6.9	1,171	6.9	4,426	6.4	1,452	6.6	10,213	6.6
Lung, trachea, and mediastinum	7,069	15.3	2,639	15.5	14,946	21.5	5,386	24.6	30,040	19.4
Lung	5,469	11.8	2,272	13.3	12,917	18.6	4,734	21.6	25,392	16.4
Breast	8,945	19.4	3,049	17.9	14,148	20.4	4,119	18.8	30,261	19.6
Liver, biliary tract, pancreas	1,936	4.2	713	4.2	2,742	3.9	964	4.4	6,355	4.1
Gastric, small intestine, colorectal	1,897	4.1	806	4.7	3,742	5.4	1,399	6.4	7,844	5.1
Gynecologic	3,253	7.0	1,156	6.8	3,405	4.9	855	3.9	8,669	5.6
Urogenital	5,544	12.0	2,043	12.0	8,068	11.6	2,905	13.3	18,560	12.0
Prostate	4,290	9.3	1,385	8.1	5,627	8.1	1,916	8.8	13,218	8.6
Hematopoietic and lymphatic	2,460	5.3	1,052	6.2	3,624	5.2	904	4.1	8,040	5.2
Skin, bone, and soft tissue	1,607	3.5	749	4.4	1,830	2.6	1,018	4.6	5,204	3.4
Other (malignant)	705	1.5	235	1.4	822	1.2	313	1.4	2,075	1.3
Benign tumors	664	1.4	268	1.6	1,289	1.9	135	0.6	2,356	1.5
Pediatric <15 y (included in totals above)	435	0.9	123	0.7	187	0.3	302	1.4	1,047	0.7
Total	46,165	100	17,023	100	69,506	100	21,895	100	154,589[†]	(100)

Abbreviations as in Table 2.

*Number of total number of new patients different with these data, because no data on primary sites were reported by some institutions.

Table 6. Distribution of specific treatments and numbers of patients treated with these modalities by PCS stratification of institutions

Specific therapy	A1 ($n = 66$)		A2 ($n = 67$)		B1 ($n = 290$)		B2 ($n = 289$)			Total ($n = 712$)	
	n	%	n	%	n	%	n	%	p	n	%
Intracavitary RT (n)									<0.0001		
Treatment facilities	61	92.4	37	55.2	71	24.5	12	4.2		181	25.4
Cases	1,670		527		974		75			3,246	
Interstitial RT									<0.0001		
Treatment facilities	42	63.6	14	20.9	18	6.2	5	1.7		79	11.1
Cases	1,818		286		638		31			2,773	
Radioactive iodine therapy for prostate cancer									<0.0001		
Treatment facilities	25	37.9	6	9.0	7	2.4	1	0.3		39	5.5
Cases	1,166		152		430		17			1,765	
Total body RT									<0.0001		
Treatment facilities	60	90.9	36	53.7	78	26.9	17	5.9		191	26.8
Cases	706		237		687		108			1,738	
Intraoperative RT									<0.0001		
Treatment facilities	23	34.8	12	17.9	20	7.0	11	3.8		66	9.3
Cases	212		39		111		25			387	
Stereotactic brain RT									<0.0001		
Treatment facilities	46	69.7	31	46.3	91	31.4	29	10.0		197	27.7
Cases	1,680		482		8,513		447			11,122	
Stereotactic body RT									<0.0001		
Treatment facilities	31	50.0	14	20.9	36	12.4	11	3.8		92	12.9
Cases	482		263		679		234			1,658	
IMRT									<0.0001		
Treatment facilities	16	24.2	4	6.0	12	4.1	1	0.3		33	4.6
Cases	426		67		212		50			755	
Thermoradiotherapy									0.0004		
Treatment facilities	10	15.2	4	6.0	15	5.2	7	2.4		36	5.1
Cases	339		27		134		81			581	

Abbreviations: PCS = Patterns of Care Study; RT = radiotherapy; IMRT = intensity-modulated radiotherapy.

problems with their quality of care, a drastic reform of our current medical care systems is required. However, great care is needed to ensure that the long-term success of radiation oncology in Japan and patient benefits are well balanced with the costs. Even under the current conditions, however, the number of FTE ROs increased by 2.1 times compared with the number in 1990 (3). However, the patient load/FTE RO also increased by 1.4 times to 247 during the same period, perhaps reflecting the growing popularity of RT because of recent advances in technology and improvement in clinical results. This caseload ratio in Japan has already exceeded the limit of the Blue Book guidelines of 200 patients/RO (15, 16). The percentage of distribution of institutions by patient load/RO showed a slightly smaller distribution than that of the United States in 1989 (3). Therefore, Japanese radiation oncology seems to be catching up quickly

with the western system despite limited resources. Furthermore, additional recruiting and education of ROs are now top priorities of the JASTRO.

The distribution of patient load/RT technologists showed that 13% of institutions met the narrow guideline range (100–120/RT technologist), and the rest were densely distributed around the peak. Compared with the distribution in the United States in 1989, >20% of institutions in Japan had a relatively low caseload of 10–60 because a large number of smaller B2-type institutions still accounted for nearly 40% of institutions exceeding the range of the guidelines. As for medical physicists, a similar analysis for patient load/FTE staff was difficult, because the number was still small, and they were working mainly in metropolitan areas. In Japan, radiation technologists have been acting as medical physicists, so that their education has been changed from 3 to 4 years

Table 7. Brain metastasis or bone metastasis patients treated with RT in 2005 by PCS institutional stratification

	Patients					
Metastasis	A1 ($n = 66$)	A2 ($n = 67$)	B1 ($n = 290$)	B2 ($n = 289$)	p	Total ($n = 712$)
Brain	2,565 (4.7)	1,204 (5.6)	9,774 (11.0)	1,778 (6.8)	<0.0001	15,321 (8.0)
Bone	6,243 (11.4)	2,845 (13.3)	13,331 (15.0)	5,057 (19.4)	<0.0001	27,476 (14.4)

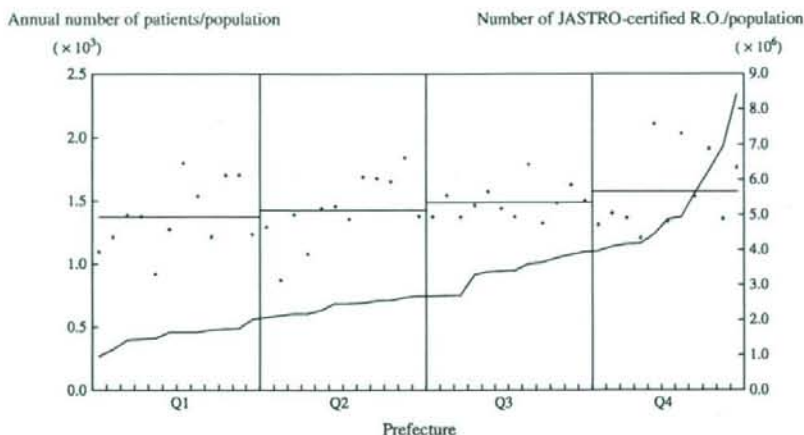Data presented as number of patients, with percentages in parentheses.

Fig. 3. Geographic distribution for 47 prefectures of annual number of patients (new plus repeat) per 1,000 population arranged in order of increasing number of Japanese Society of Therapeutic Radiation Oncology (JASTRO)-certified radiation oncologists (RO)/1,000,000 population by prefecture. Q1, 0–25%; Q2, 26–50%; Q3, 51–75%; and Q4, 76–100%. Horizontal bar shows average annual number of patients (new plus repeat) per 1,000 population of prefectures per quarter.

during the past decade and graduate and postgraduate courses have been introduced. Currently, those who have obtained a master's degree or radiation technologists with enough clinical experience can take the examination for qualification as a medical physicist, as can those with a master's degree in science or engineering, like those in the United States or Europe. In Japan, a unique education system for medical physicists might be developed because the anticancer law actively supports improvements in quality assurance/quality control specialization for RT. However, the validity of this education and training system remains unsatisfactory, because we are still in the trial-and-error stage.

The distribution of the primary site for RT showed that more lung cancer patients were treated in B1 or B2 nonacademic institutions and more head-and-neck cancer patients were treated in A1 or A2 academic institutions. These findings might be because more curative patients were referred to academic institutions and more palliative patients with lung cancer were treated in nonacademic institution in Japan. In addition, more patients with bone metastasis were treated in nonacademic institutions. The use of specific treatments and the number of patients treated with these modalities were significantly affected by institutional stratification, with more specific treatments performed at academic institutions. These findings indicate that significant differences in the patterns of care, as reflected in the structure, process, and, possibly, outcomes for cancer patients still exist in Ja-

pan. These differences point to opportunities for improvement. We, therefore, based the Japanese Blue Book guidelines on this stratification by the PCS data (16) and are now in preparing to revise them accordingly.

The geographic patterns demonstrated significant differences among the prefectures in the use of RT, ranging from 0.9 to 2.1 patients/1,000 population. Furthermore, the number of JASTRO-certified physicians/population might be associated with the use of RT, so that a shortage of ROs or medical physicists on a regional basis will remain a major concern in Japan. The JASTRO has been making every effort to recruit and educate ROs and medical physicists through public relations, training courses, involvement in the national examination for physicians, and seeking to increase the reimbursement by the government-controlled insurance program, and other actions.

CONCLUSION

The Japanese structure of radiation oncology has clearly improved during the past 15 years in terms of equipment and its functions, although a shortage of manpower and differences in maturity by type of institution and caseload remain. Structural immaturity is an immediate target for improvement, and, for improvements in process and outcome, the PCS or National Cancer Database, which are currently operational and being closely examined, can be expected to play an important role in the future.

REFERENCES

1. Owen JB, Coia LR, Hanks GE. Recent patterns of growth in radiation therapy facilities in the United States: A Patterns of Care Study report. *Int J Radiat Oncol Biol Phys* 1992;24: 983–986.
2. Tsunemoto H, for the Japanese Society of Therapeutic Radiology and Oncology (JASTRO). Present status of Japanese radia-

tion oncology: National survey of structure in 1990 (in Japanese). Tokyo: Japanese Society of Therapeutic Radiology and Oncology, 1992.
3. Teshima T, Owen JB, Hanks GE, *et al.* A comparison of the structure of radiation oncology in the United States and Japan. *Int J Radiat Oncol Biol Phys* 1996;34:235–242.